Contact mechanics and elements of tribology

Lecture 5

Contact at small scales

Vladislav A. Yastrebov

Mines Paris - PSL, CNRS
Centre des Matériaux, Evry, France

@ Centre des Matériaux (& virtually)
February 25, 2025

Outline

Objective:

link **roughness** parameters with the evolution of the true **contact area**

Contact between rough surfaces

Contact under microscope

Contact under microscope

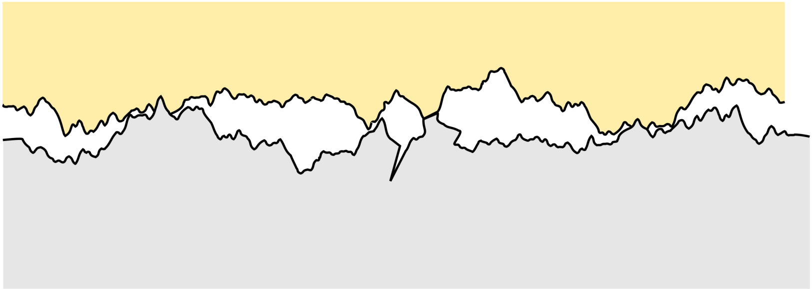

Problem statement & methods

Problem

- Solve contact problem for two elastic half-spaces E_1, ν_1 and E_2, ν_2
- With surface roughnesses $z_1(x,y)$ and $z_2(x,y)$
- Balance of momentum $\nabla \cdot \underline{\underline{\sigma}} = 0$,
- Boundary conditions $-\sigma_z^\infty = p_0$
- Contact constraints $g \geq 0, \quad p \geq 0, \quad g\,p = 0$,
  where $g(x,y)$ is the gap between surfaces,
  $p = -\underline{n} \cdot \underline{\underline{\sigma}} \cdot \underline{n}$ is the contact pressure.

Methods

- Finite element method

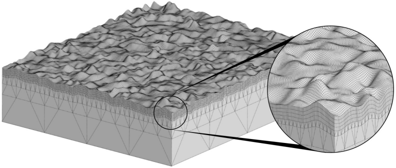

[1] Yastrebov, Wiley/ISTE (2013)

- Boundary element method

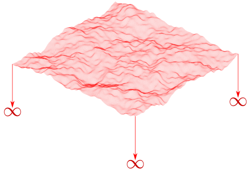

[2] Stanley & Kato, J Tribol 119 (1997)

Problem mapping

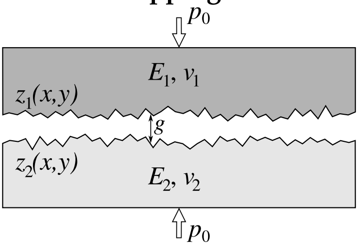

- **Flat** elastic[1] half-space with $E^* = \dfrac{E_1 E_2}{E_2(1-\nu_1^2) + E_1(1-\nu_2^2)}$
- **Rough** rigid[1] surface with $z^* = z_2 - z_1$
- Optimization problem[2]: $\min \mathcal{F}$

  under constraints $p \geq 0$ and $\frac{1}{A_0}\int\limits_A p dA = p_0$,

  with $\mathcal{F} = \int\limits_A p[u_z/2 + g]dA$, vertical displacement u_z and gaps g

[1] Barber, Bounds on the electrical resistance between contacting elastic rough bodies, PRSL A 459 (2003)
[2] Kalker, Variational Principles of Contact Elastostatics, J Inst Maths Applics (1977)

Problem mapping

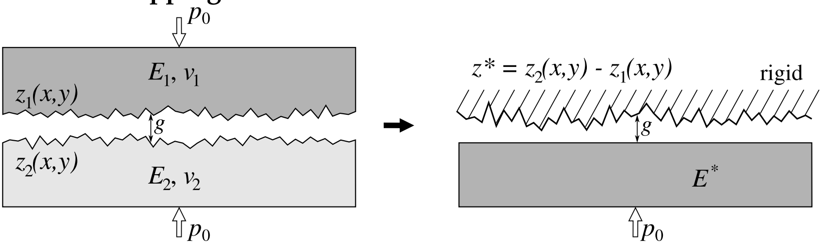

- **Flat** elastic[1] half-space with $E^* = \dfrac{E_1 E_2}{E_2(1-\nu_1^2) + E_1(1-\nu_2^2)}$
- **Rough** rigid[1] surface with $z^* = z_2 - z_1$
- Optimization problem[2]: $\min \mathcal{F}$

  under constraints $p \geq 0$ and $\frac{1}{A_0} \int\limits_A p dA = p_0$,

  with $\mathcal{F} = \int\limits_A p[u_z/2 + g]dA$, vertical displacement u_z and gaps g

[1] Barber, Bounds on the electrical resistance between contacting elastic rough bodies, PRSL A 459 (2003)
[2] Kalker, Variational Principles of Contact Elastostatics, J Inst Maths Applics (1977)

Analytical models

Multi-asperity models

[1] Greenwood, Williamson. *P Roy Soc Lond A Mat* (1966)
[2] Bush, Gibson, Thomas. *Wear* (1975)
[3] Mc Cool. *Wear* (1986)
[4] Thomas. *Rough Surfaces* (1999)
[5★] Greenwood. *Wear* (2006)
[6] Carbone. *J. Mech. Phys. Solids* (2009)
[7] Ciavarella, Greenwood, Paggi. *Wear* (2008)

Persson's model

[8] Persson. *J. Chem. Phys.* (2001)
[9] Persson. *Phys. Rev. Lett.* (2001)
[10] Persson, Bucher, Chiaia. *Phys. Rev. B* (2002)
[11] Müser. *Phys. Rev. Lett.* (2008)

Cross-link studies

[12] Manners, Greenwood. *Wear* (2006)
[13] Carbone, Bottiglione. *J. Mech. Phys. Solids* (2008)
[14] Paggi, Ciavarella. *Wear* (2010)

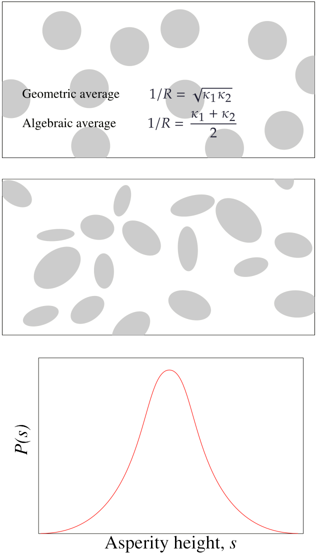

Fig. Multi-asperity models

Analytical models

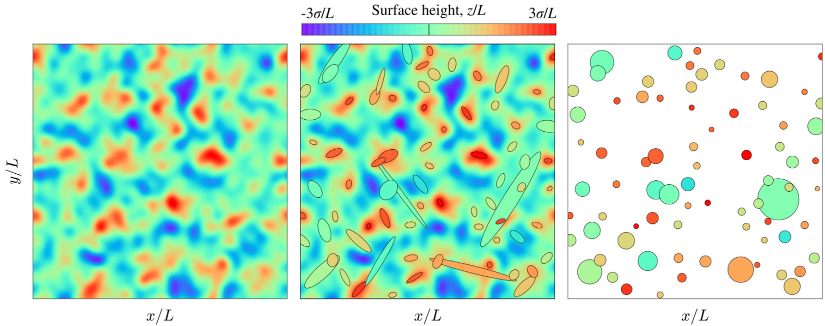

Fig. Roughness and detected asperities for $L/\lambda_l = 4$ and $L/\lambda_s = 16$

Analytical models

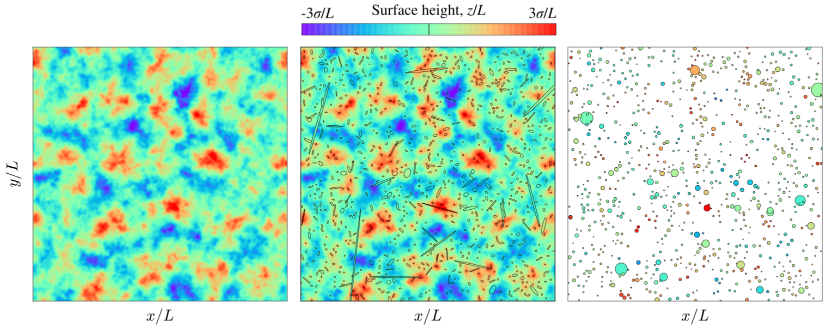

Fig. Roughness and detected asperities for $L/\lambda_l = 4$ and $L/\lambda_s = 64$

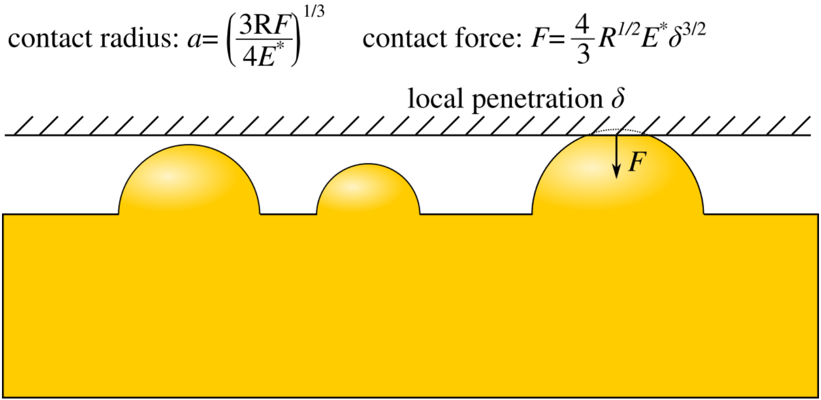

Fig. Hertz's theory of contact

Analytical models

Multi-asperity models

[1] Greenwood, Williamson. *P Roy Soc Lond A Mat* (1966)
[2] Bush, Gibson, Thomas. *Wear* (1975)
[3] Mc Cool. *Wear* (1986)
[4] Thomas. *Rough Surfaces* (1999)
[5★] Greenwood. *Wear* (2006)
[6] Carbone. *J. Mech. Phys. Solids* (2009)
[7] Ciavarella, Greenwood, Paggi. *Wear* (2008)

Persson's model

[8] Persson. *J. Chem. Phys.* (2001)
[9] Persson. *Phys. Rev. Lett.* (2001)
[10] Persson, Bucher, Chiaia. *Phys. Rev. B* (2002)
[11] Müser. *Phys. Rev. Lett.* (2008)

Cross-link studies

[12] Manners, Greenwood. *Wear* (2006)
[13] Carbone, Bottiglione. *J. Mech. Phys. Solids* (2008)
[14] Paggi, Ciavarella. *Wear* (2010)

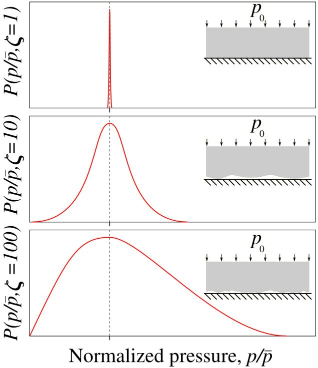

Fig. Persson's model

$$\frac{\partial P(p,\zeta)}{\partial V(\zeta)} = \frac{1}{2}\frac{\partial^2 P(p,\zeta)}{\partial p^2} \qquad P(0,\zeta) = 0$$

$$V(\zeta) = \frac{1}{2}E^* m_2(\zeta) = \frac{\pi E^*}{2}\int_{k_l}^{\zeta k_l} k^3 \Phi^p(k)dk$$

Why is the sky dark at night?

Why is the sky dark at night?

- Olbers' paradox or "dark night sky paradox"
- Two nominally-flat elastic half-spaces in contact
- At small scale they are rough with asperity density D
- Vertical displacement decay $u_z \sim 1/r$
- At every asperity, force F
- Sum up displacements induced by all forces*

$$u_z \sim \int\limits_0^{2\pi}\int\limits_{r_0}^{R} \frac{F}{r} r\,dr\,d\phi \xrightarrow[R\to\infty]{} \infty$$

---

*In case of light intensity I, it decays as $1/r^2$ but the integral is in volume for a constant star density the integral light intensity is:

$$\mathcal{I} \sim \int\limits_0^{2\pi}\int\limits_0^{\pi/2}\int\limits_{r_0}^{R} \frac{I}{r^2} \underbrace{r^2\sin(\theta)\,dr\,d\phi d\theta}_{\text{Volume element}} \xrightarrow[R\to\infty]{} \infty$$

Comparison of models

Multi-asperity models **Persson's model**

1. Evolution of the real contact area $A(p_0)$ for $A/A_0 \to 0$

$$\frac{A}{A_0} = \frac{\kappa}{\sqrt{\langle|\nabla z|^2\rangle}}\frac{p_0}{E^*}$$

$\kappa_{BGT} = \sqrt{2\pi} \approx 2.5$ *according to* [2-5]

$\kappa_P = \sqrt{8/\pi} \approx 1.6$ *according to* [6-7]

2. Evolution of the real contact area $A(p_0)$ for $\forall A/A_0$

$\frac{A}{A_0} = A(p_0, \alpha)/A_0$ *according to* [2-5]

$\frac{A}{A_0} = \mathrm{erf}\left(\sqrt{\frac{2}{\langle|\nabla z|^2\rangle}}\frac{p_0}{E^*}\right)$ *according to* [6-7]

[1] Greenwood, Williamson, P Roy Soc Lond A Mat 295 (1966)
[2] Bush, Gibson, Thomas, Wear 35 (1975)
[3] Mc Cool, Wear 107 (1986)
[4] Thomas, Rough Surfaces (1999)
[5] Greenwood, Wear 261 (2006)
[6] Persson, J. Chem. Phys. 115 (2001)
[7] Persson, Phys. Rev. Lett. 87 (2001)
[8] Persson, Bucher, Chiaia, Phys. Rev. B 65 (2002)
[9] Müser, Phys. Rev. Lett. 100, (2008)

Simulations set-up

- Cut-off parameters: $L/\lambda_l \otimes L/\lambda_s = \{1, 2, 4, 8, 16\} \otimes \{32, 64, 128, 256, 512\}$
- Hurst exponent $H = \{0.4, 0.8\}$
- 10 random surface realizations per combination of parameters
- Discretization: $\{L/\Delta x\} \times \{L/\Delta x\} = 2048 \times 2048$
- Search for contact area A', gap field $g(x, y)$ and gap PDF $P(g)$

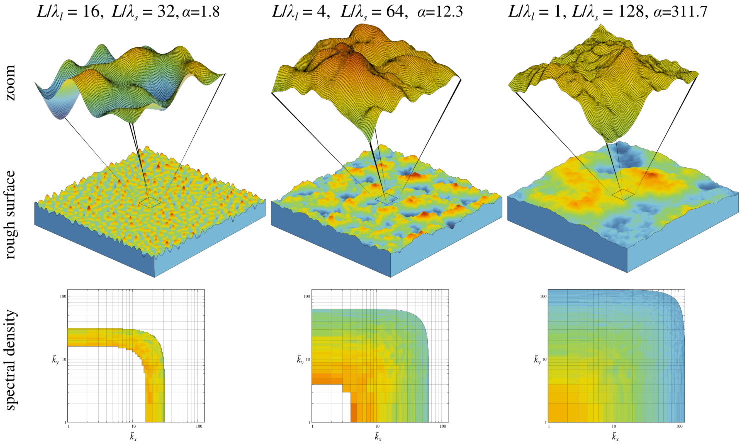

Contact area and contact pressure evolution

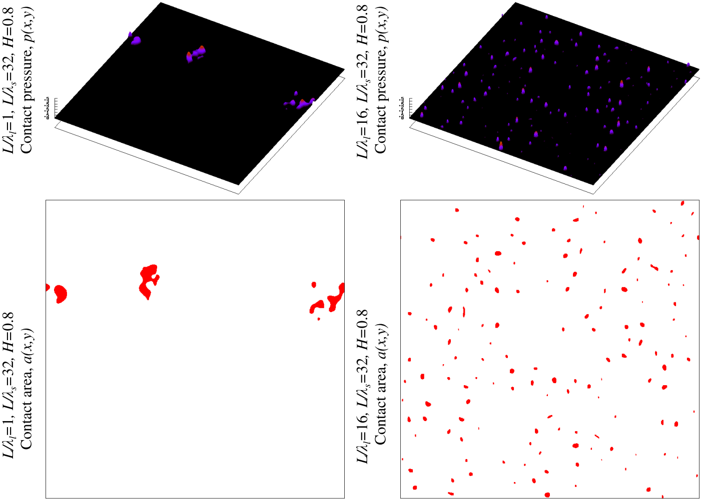

Contact area and contact pressure evolution

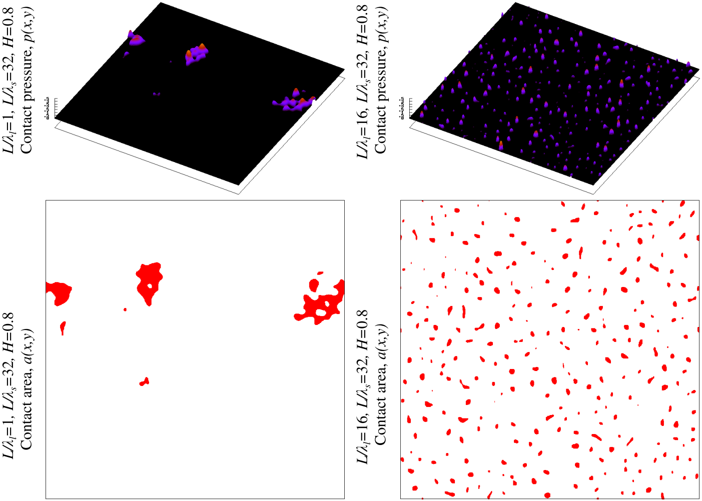

Contact area and contact pressure evolution

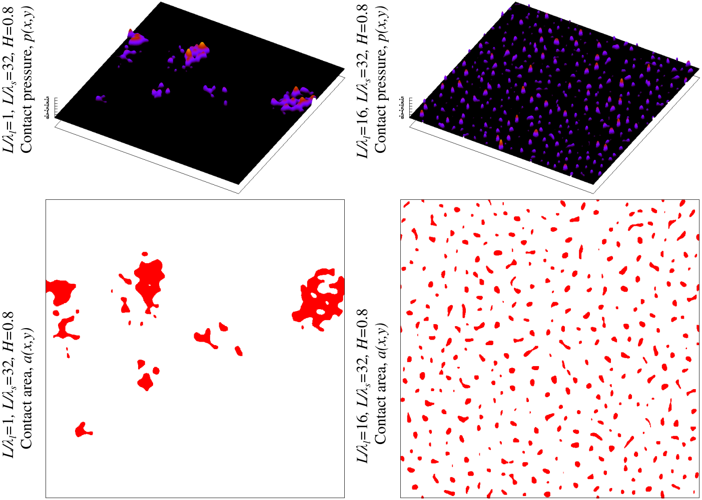

Contact area and contact pressure evolution

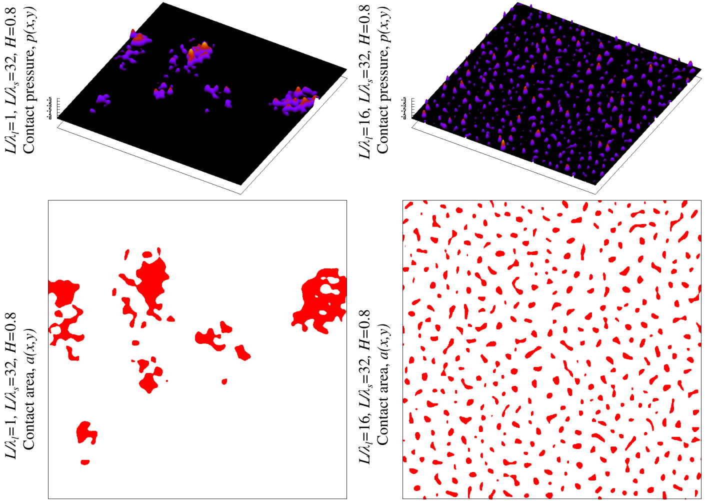

Contact area and contact pressure evolution

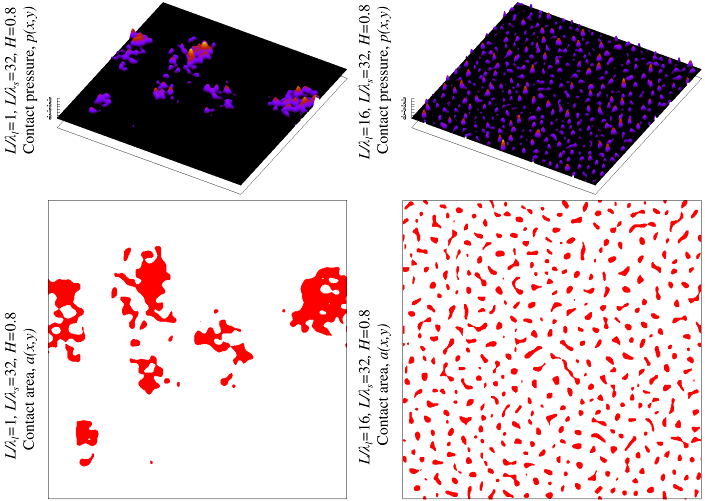

Contact area and contact pressure evolution

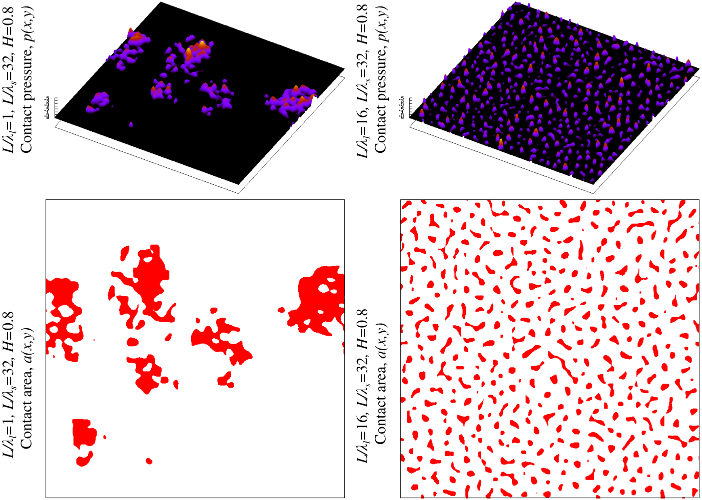

Contact area and contact pressure evolution

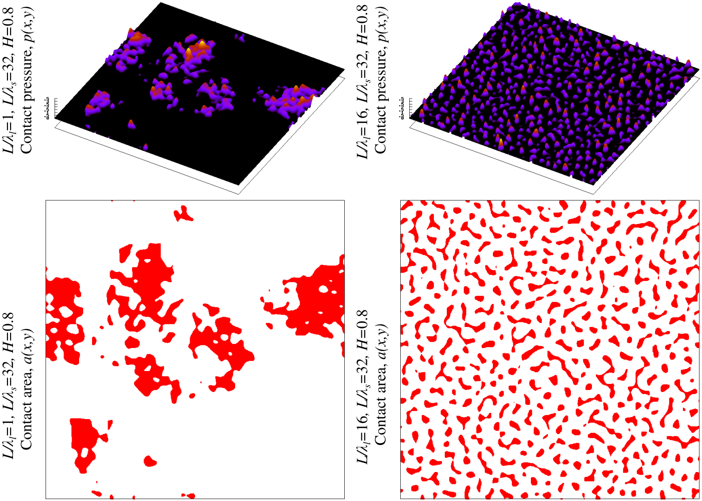

Contact area and contact pressure evolution

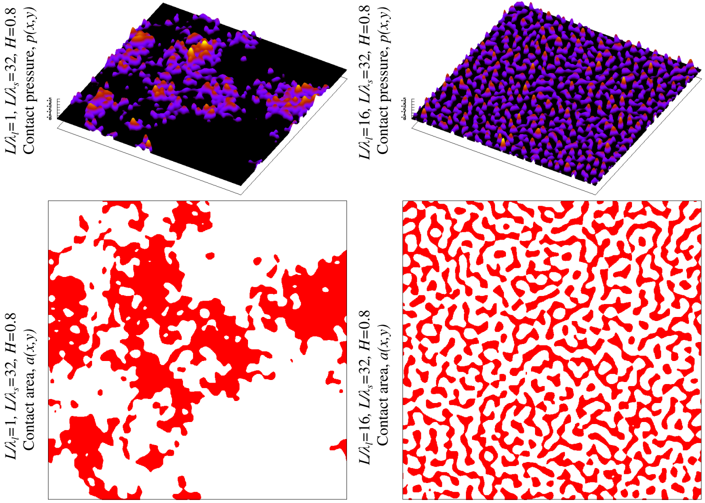

Contact area and contact pressure evolution

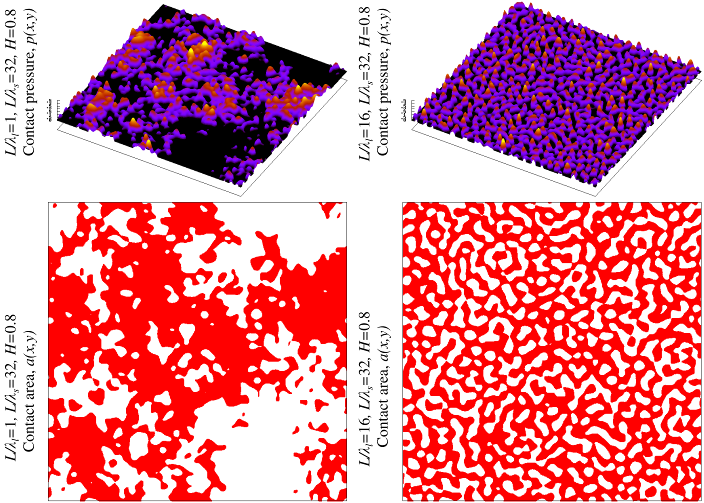

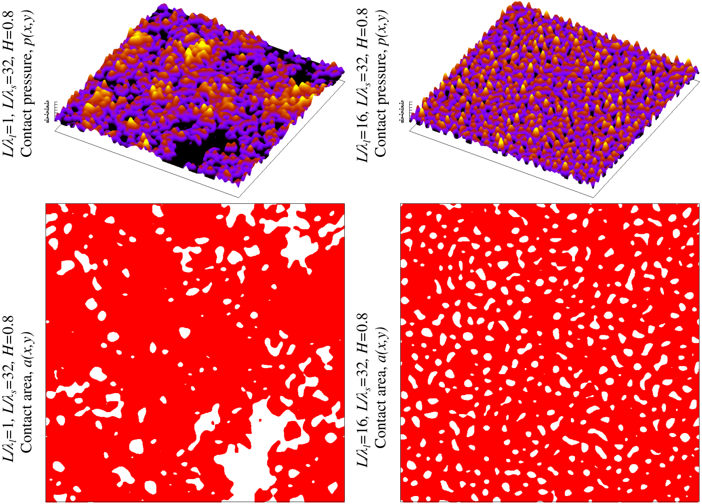

L/λl=1, L/λs=32, H=0.8
Contact pressure, p(x,y)
L/λl=16, L/λs=32, H=0.8
Contact pressure, p(x,y)
L/λl=1, L/λs=32, H=0.8
Contact area, a(x,y)
L/λl=16, L/λs=32, H=0.8
Contact area, a(x,y)

Contact area and contact pressure evolution

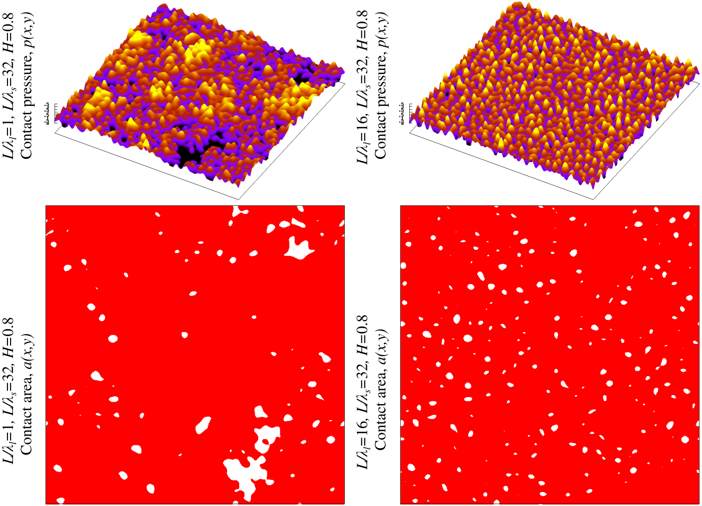

Contact area and contact pressure evolution

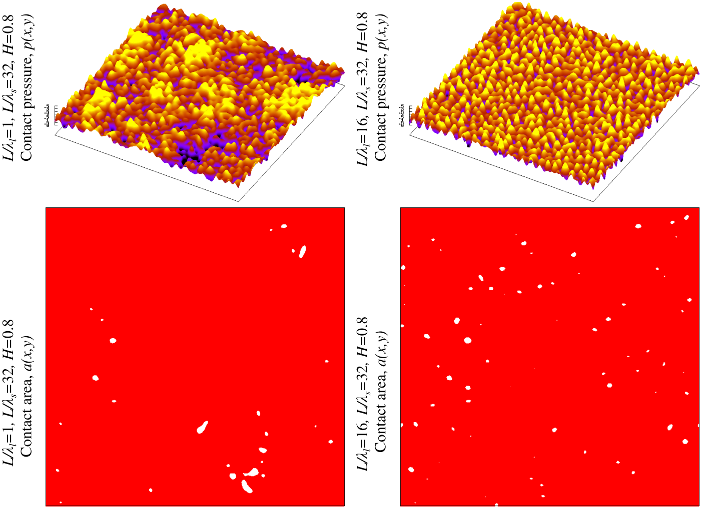

Contact area and contact pressure evolution

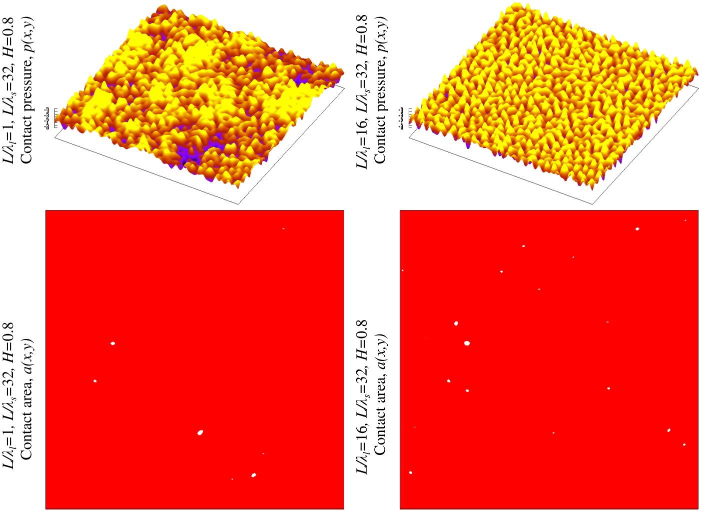

Contact area and contact pressure evolution

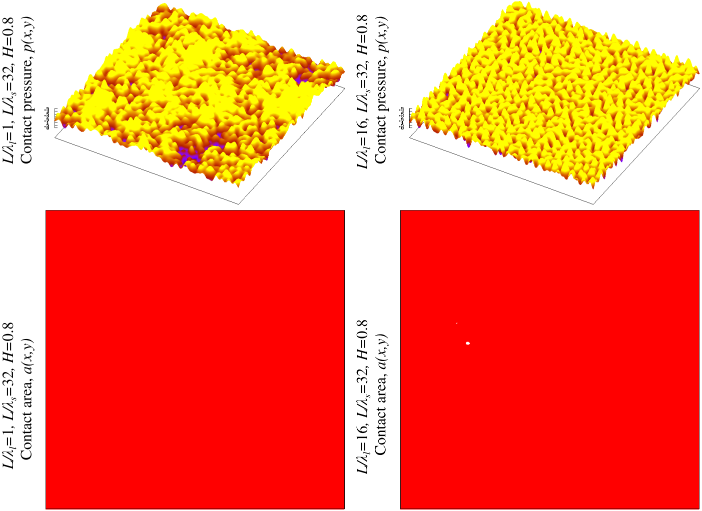

Results: contact area

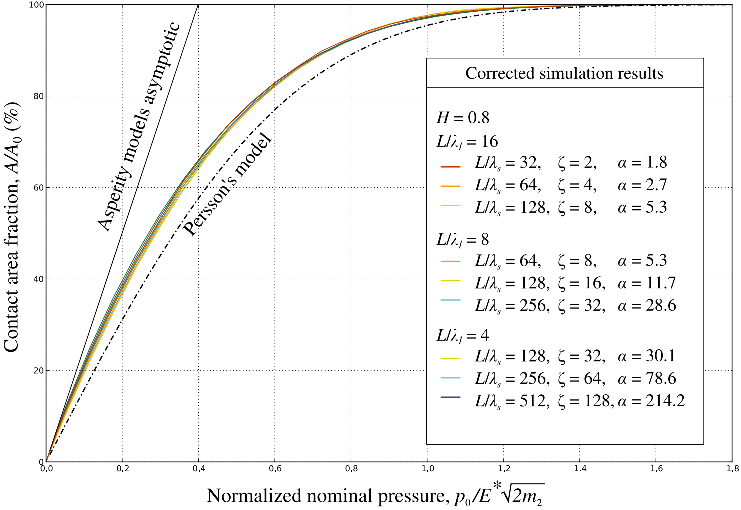

Multi-asperity models asymptotic[1,2], Persson's model[3]

[1] Bush, Gibson, Thomas, Wear 35 (1975), [2] Carbone, Bottiglione. *J. Mech. Phys. Solids* (2008), [3] Persson. *J. Chem. Phys.* (2001)

Results: contact area

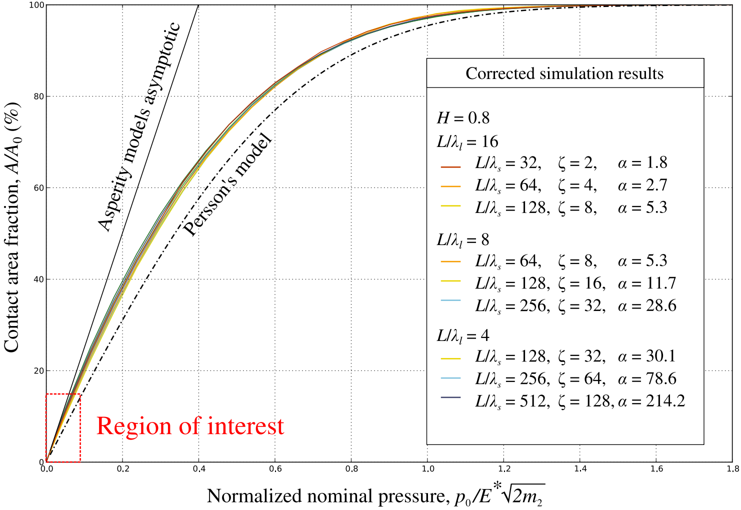

Multi-asperity models asymptotic[1,2], Persson's model[3]

[1] Bush, Gibson, Thomas, Wear 35 (1975), [2] Carbone, Bottiglione. *J. Mech. Phys. Solids* (2008), [3] Persson. *J. Chem. Phys.* (2001)

Real contact area: interpretation of results?

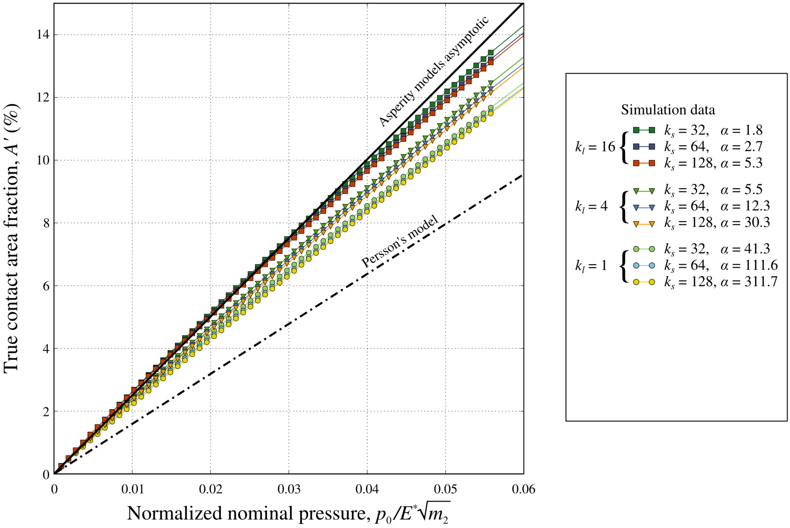

Raw data

[1] Yastrebov, Anciaux, Molinari, Int J Solids Struct 52 (2015)

Numerical error correction

- Contact area is overestimated in simulations:

  $A_{\text{sim}} > A_*$

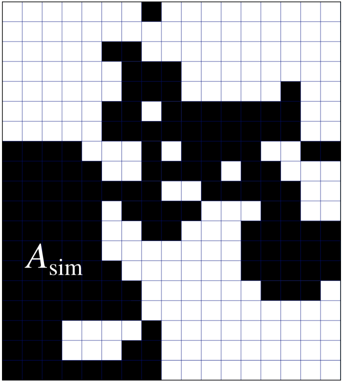

Numerical error correction

- Contact area is overestimated in simulations:

$$A_{\text{sim}} > A_*$$

- The overestimation is localized at boundary nodes:

$$A_{\text{sim}} > A_* > A_{\text{sim}}^{\text{int}}$$

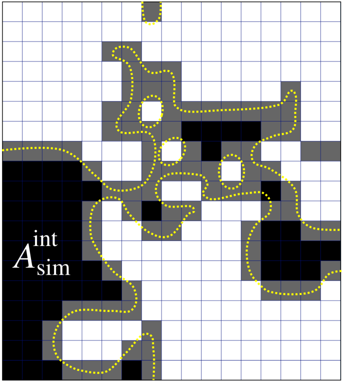

Numerical error correction

- Contact area is overestimated in simulations:

  $$A_{\text{sim}} > A_*$$

- The overestimation is localized at boundary nodes:

  $$A_{\text{sim}} > A_* > A^{\text{int}}_{\text{sim}}$$

- Boundary area ~ perimeter S_d:

  $$A_{\text{sim}} - A^{\text{int}}_{\text{sim}} = S_d \Delta x$$

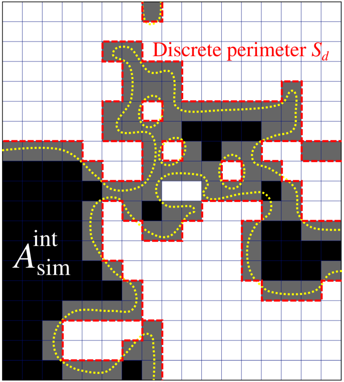

Numerical error correction

- Contact area is overestimated in simulations:

  $$A_{\text{sim}} > A_*$$

- The overestimation is localized at boundary nodes:

  $$A_{\text{sim}} > A_* > A_{\text{sim}}^{\text{int}}$$

- Boundary area ~ perimeter S_d:

  $$A_{\text{sim}} - A_{\text{sim}}^{\text{int}} = S_d \Delta x$$

- Manhattan S_d vs Euclidean metric S:

  $$\langle S \rangle = \frac{\pi}{4} \langle S_d \rangle$$

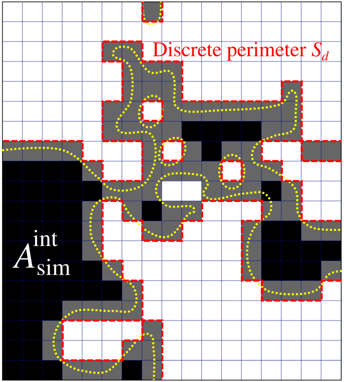

Numerical error correction

- Contact area is overestimated in simulations:

  $$A_{\text{sim}} > A_*$$

- The overestimation is localized at boundary nodes:

  $$A_{\text{sim}} > A_* > A_{\text{sim}}^{\text{int}}$$

- Boundary area ∼ perimeter S_d:

  $$A_{\text{sim}} - A_{\text{sim}}^{\text{int}} = S_d \Delta x$$

- Manhattan S_d vs Euclidean metric S:

  $$\langle S \rangle = \frac{\pi}{4} \langle S_d \rangle$$

- True contact area estimation:

$$\boxed{A_* \approx A_{\text{sim}} - \beta \frac{\pi}{4} S_d \Delta x}$$

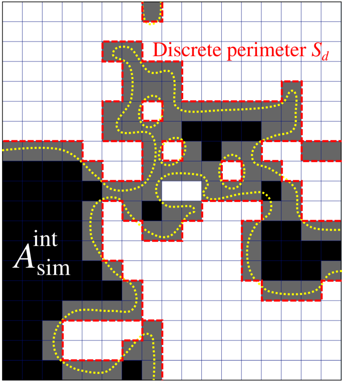

Numerical error correction: corrective factor

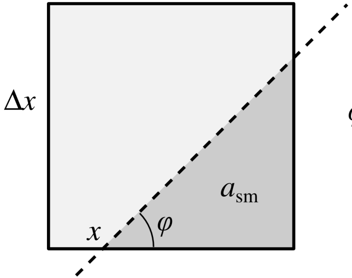

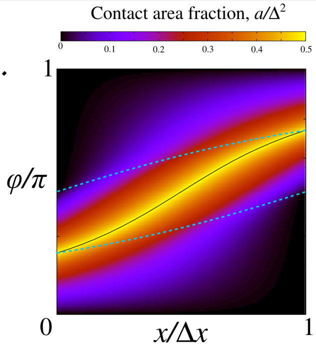

Corrective factor $\beta = \dfrac{\langle a_{\mathrm{sm}}\rangle}{\Delta x^2} = \dfrac{1}{\Delta x^2}\int\limits_0^h \int\limits_0^\pi a_{\mathrm{sm}} P(x,\phi)\,dx d\phi = \dfrac{\pi - 1 + \ln 2}{6\pi}$

$$\beta = 0.150387618994810151606955\ldots$$

True area estimation: $\boxed{A_* \approx A_{\mathrm{sim}} - \dfrac{\pi - 1 + \ln 2}{24} S_d \Delta x}$

Numerical error correction: convergence study

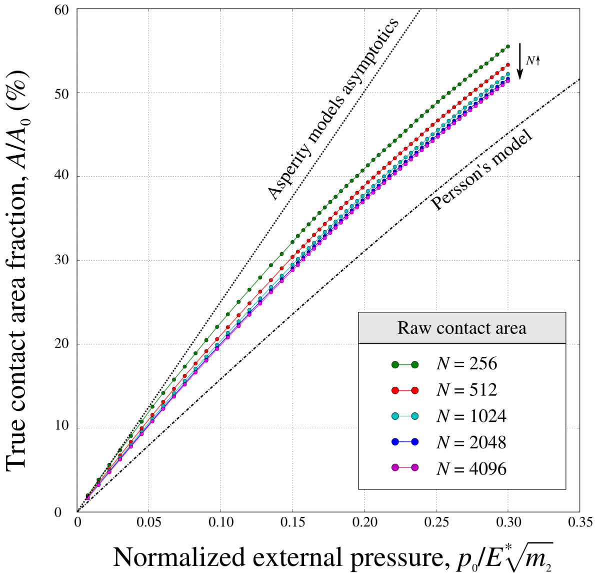

[1] Yastrebov, Anciaux, Molinari, Tribol Int 114 (2017)

Numerical error correction: convergence study

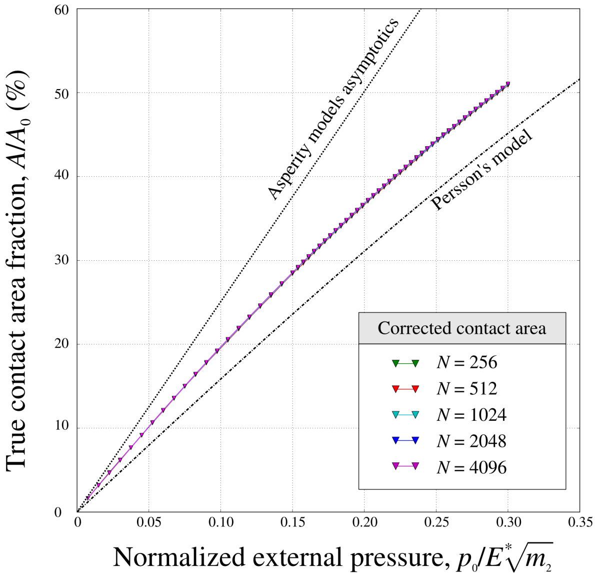

[1] Yastrebov, Anciaux, Molinari, Tribol Int 114 (2017)

Morphological correction

- Morphology of contact clusters

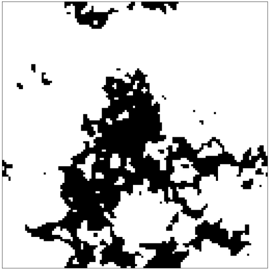

N=128, raw

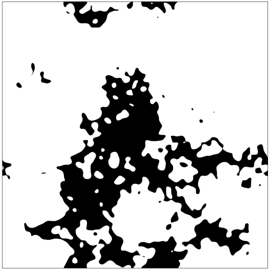

N=2048, raw

Morphological correction

- Morphology of contact clusters

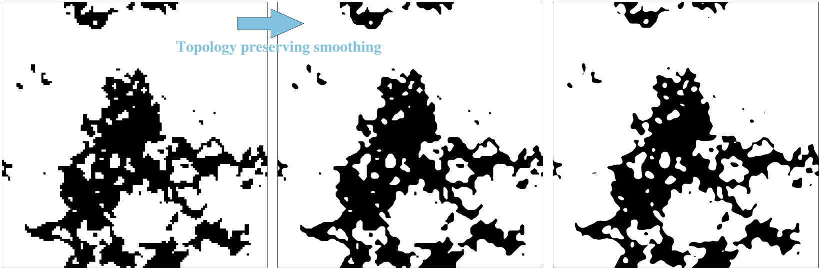

N=128, raw | N=128, smoothed | N=2048, raw

Topologically preserving smoothing results in realistic cluster geometry

[1] Couprie & Bertrand, *J Electr Imag* 13 (2004)

Real contact area: accurate results

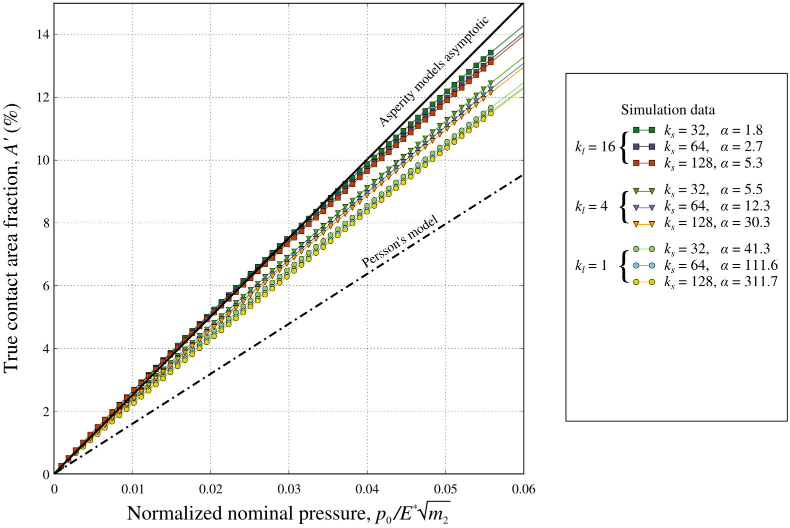

Raw data

[1] Yastrebov, Anciaux, Molinari, Int J Solids Struct 52 (2015)

Real contact area: accurate results

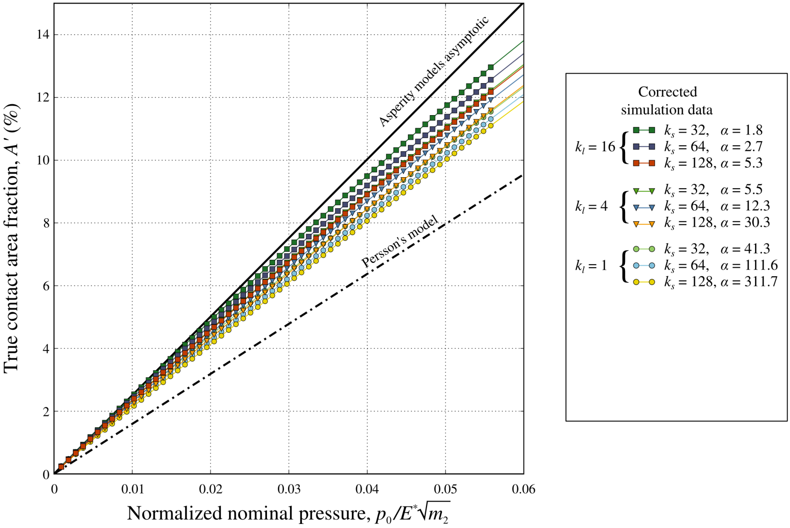

Corrected data

[2] Yastrebov, Anciaux, Molinari, *J Mech Phys Solids* 107 (2017)

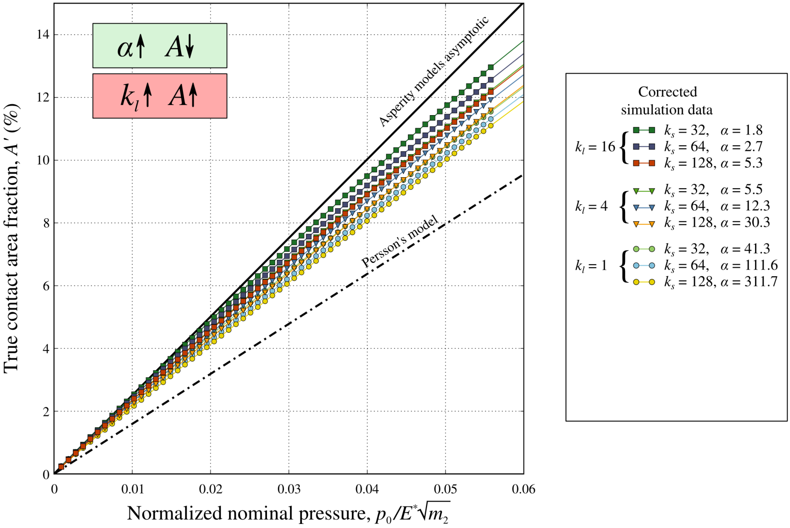

Corrected data

[2] Yastrebov, Anciaux, Molinari, *J Mech Phys Solids* 107 (2017)

Real contact area: accurate results

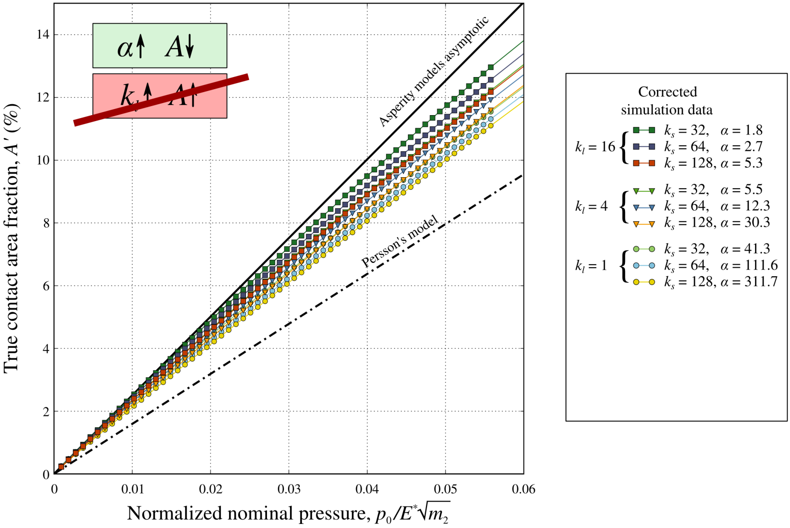

Corrected data

[2] Yastrebov, Anciaux, Molinari, *J Mech Phys Solids* 107 (2017)

Results: contact area

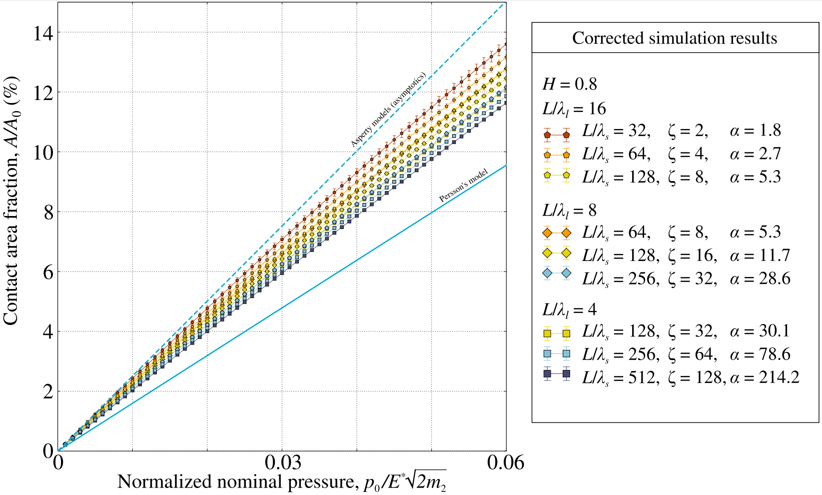

Corrected contact area (discretization independent): "magic" formula[1,2]

$$A_* \approx A_{\text{sim}} - \frac{\pi-1+\ln 2}{24} S_d \Delta x,$$

where S_d is the integral **perimeter** of the contact zones.

[1] Yastrebov, Anciaux, Molinari, *Tribol. Int.* 114 (2017)
[2] Yastrebov, Anciaux, Molinari, *J Mech Phys Solids* 107 (2017)

Results: contact area

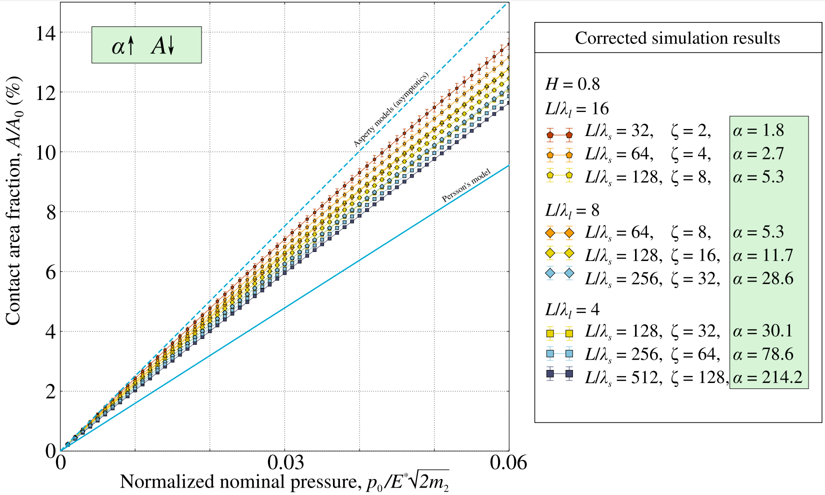

Corrected contact area (discretization independent): "magic" formula[1,2]

$$A_* \approx A_{\text{sim}} - \frac{\pi-1+\ln 2}{24} S_d \Delta x,$$

where S_d is the integral **perimeter** of the contact zones.

[1] Yastrebov, Anciaux, Molinari, *Tribol. Int.* 114 (2017)
[2] Yastrebov, Anciaux, Molinari, *J Mech Phys Solids* 107 (2017)

Role of Nayak parameter α

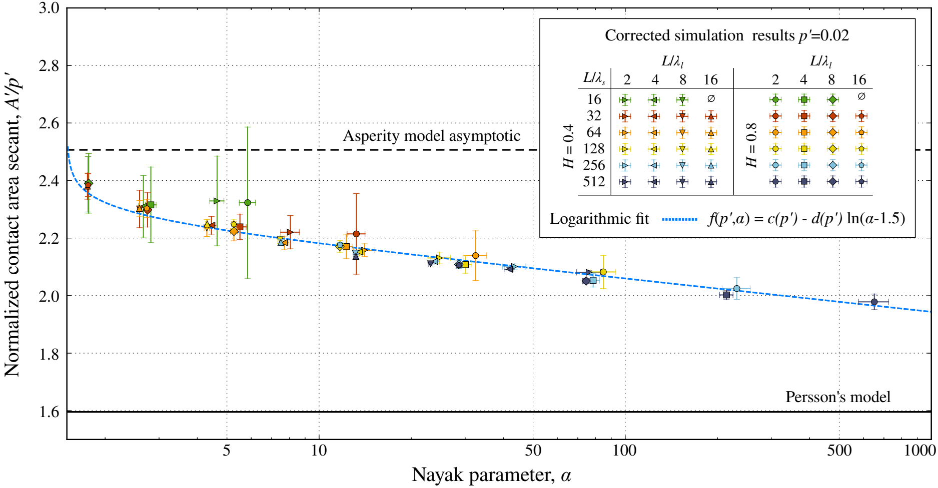

Numerical results: [1] Yastrebov, Anciaux, Molinari, J Mech Phys Solids 107 (2017)

Role of Nayak parameter α

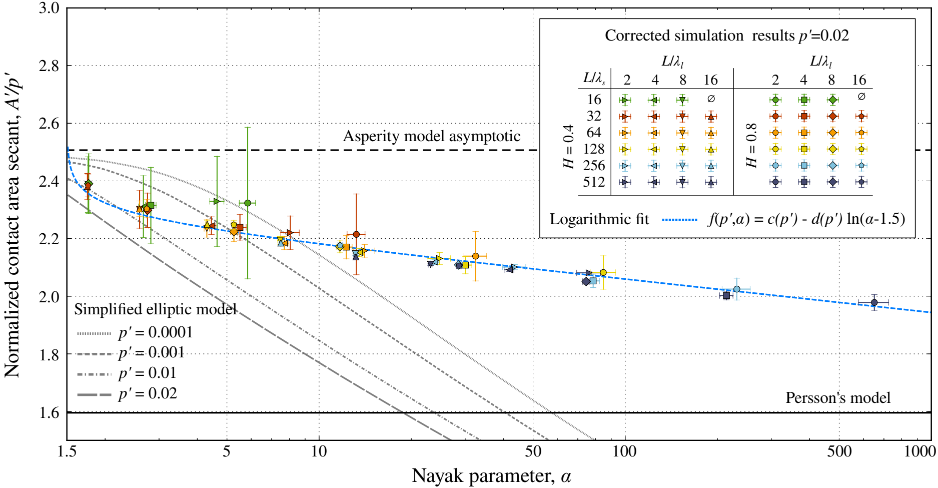

Numerical results: [1] Yastrebov, Anciaux, Molinari, J Mech Phys Solids 107 (2017)

Simplified elliptic model: [2] Greenwood, Wear (2006)

Role of Nayak parameter α

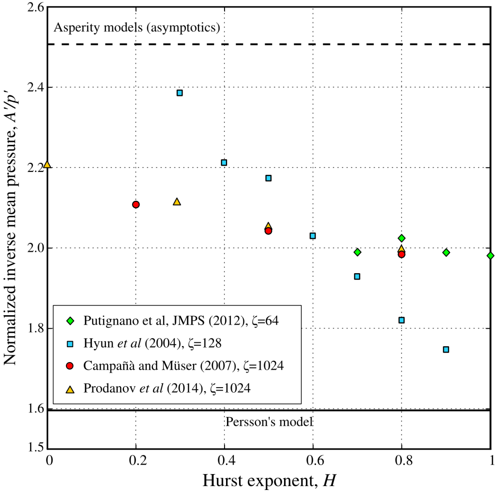

Comparison with other numerical studies
Nayak-Hurst relationship

$$\alpha(H,\zeta) = \frac{3}{2}\,\frac{(1-H)^2}{H(H-2)}\,\frac{(\zeta^{-2H}-1)(\zeta^{4-2H}-1)}{(\zeta^{2-2H}-1)^2}$$

Role of Nayak parameter α

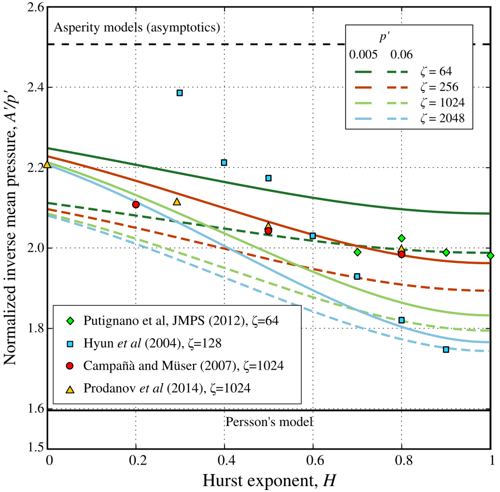

Comparison with other numerical studies
Nayak-Hurst relationship

$$\alpha(H,\zeta) = \frac{3}{2}\,\frac{(1-H)^2}{H(H-2)}\,\frac{(\zeta^{-2H}-1)(\zeta^{4-2H}-1)}{(\zeta^{2-2H}-1)^2}$$

Phenomenological relationship

- Contact area A grows with applied pressure p_0 as

$$\frac{A}{A_0} = a(\alpha)\frac{p_0}{E^*\sqrt{2m_2}} - b(\alpha)\left[\frac{p_0}{E^*\sqrt{2m_2}}\right]^2$$

- Contact area fraction $A' = A/A_0$ grows with normalized applied pressure $p' = p_0/E^*\sqrt{2m_2}$

$$\boxed{A' = a(\alpha)p' - b(\alpha)p'^2}$$

- With ≈universal adimensional constants:

$a(\alpha) = 2.35 - 0.057\ln(\alpha - 1.5)$

$b(\alpha) = 2.85 - 0.24\ln(\alpha - 1.5)$

- Pressure dependent friction coefficient:

$$\mu(p') = \mu_0\left[1 - \frac{b(\alpha)}{a(\alpha)}p'\right]$$

with $\mu_0 = a(\alpha)\tau_{max}/E^*\sqrt{2m_2}$,
τ_{max} is the maximum shear traction the contact interface can bear.

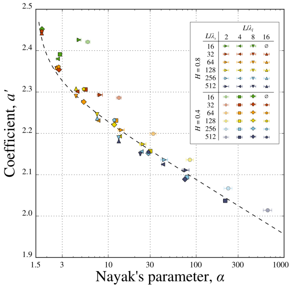

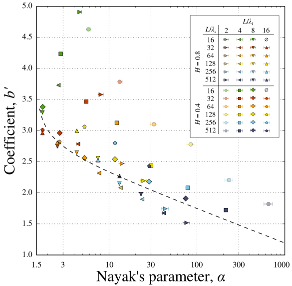

Conclusions

- Contact area growth almost linearly for small pressures and saturates at bigger pressure
- The key parameter of the contact area growth is the RMS slope or its variance $2m_2$
- Contact area depends weakly on Nayak parameter $\alpha = m_0 m_4 / m_2^2$

$$\boxed{A' = a(\alpha)p' - b(\alpha){p'}^2}$$

with $a(\alpha) = 2.35 - 0.057\ln(\alpha - 1.5), \quad b(\alpha) = 2.85 - 0.24\ln(\alpha - 1.5)$

- No effect of fractal dimension D_f *per se* on the contact area
  it affects the contact area only through the Nayak parameter

Flow through the contact interface

Problem

- **Thin creeping** flow in contact interface:
  Navier-Stokes → Stokes → Reynolds equation
- In addition: incompressible fluid, immobile walls:

$$\nabla \cdot \underline{q} = 0, \quad \underline{q} = -\frac{g^3}{12\mu}\nabla p_f$$

$\underline{q}(x,y)$ is the fluid flux,
$g(x,y)$ is the gap (opening) fields,
$p_f(x,y)$ hydrostatic fluid pressure,
μ is the dynamic viscosity.

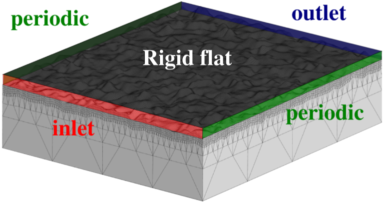

- Gap profile $g(x,y)$ for $x,y \in (0,L)$
- At inlet: $p_f = p_{\text{in}}$
- At outlet: $p_f = p_{\text{out}}$
- At lateral sides: periodic
  $q_n(y=L) = -q_n(y=0)$
- Linear problem: use FEM

Effective flow estimation

- Averaging over surface $\langle x \rangle = 1/A_0 \int_{A_0} x\, dA$ gives:

$$\langle\, \underline{q}\, \rangle = -\underline{\underline{K}}_{\text{eff}} \cdot \langle \nabla p_f \rangle$$

- For isotropic case, normalized scalar **effective transmissivity** along pressure drop OX:

$$K'_{\text{eff}} = -\frac{12\mu\langle\, q_x\, \rangle L}{m_0^{3/2}(p_{\text{in}} - p_{\text{out}})}$$

- Using effective medium[1,2] approach

$$(1 - A') \int\limits_0^\infty \frac{g^3 P(g)}{g^3 + K'_{\text{eff}} m_0^{3/2}}\, dg = \frac{1}{2}$$

$A' = A/A_0$ is the contact area fraction, $P(g)$ is the gap probability density.

[1] Kirkpatrick. Rev Modern Phys, 45 (1973)
[2] Lorenz & Persson. Europ Phys J E: Soft Matter, 31 (2010)

Danger: geometrical overlap

- Geometrical overlap model is highly inaccurate

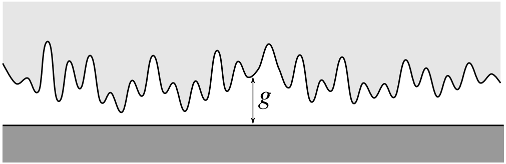

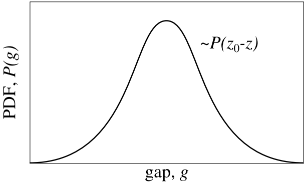

Danger: geometrical overlap

- Geometrical overlap model is highly inaccurate

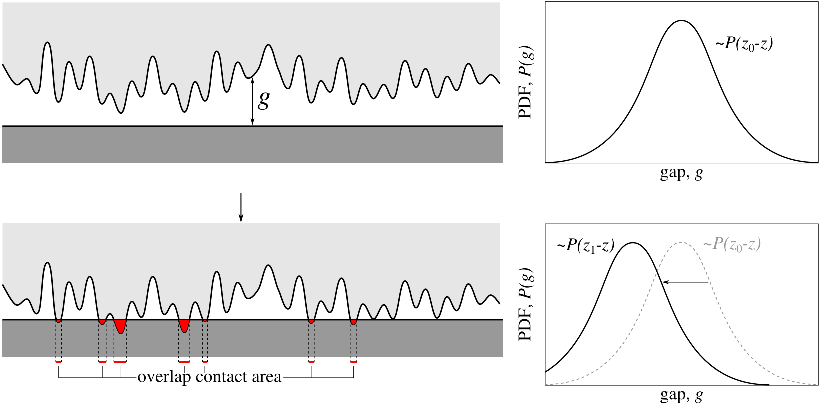

Solid contact results: gap distribution

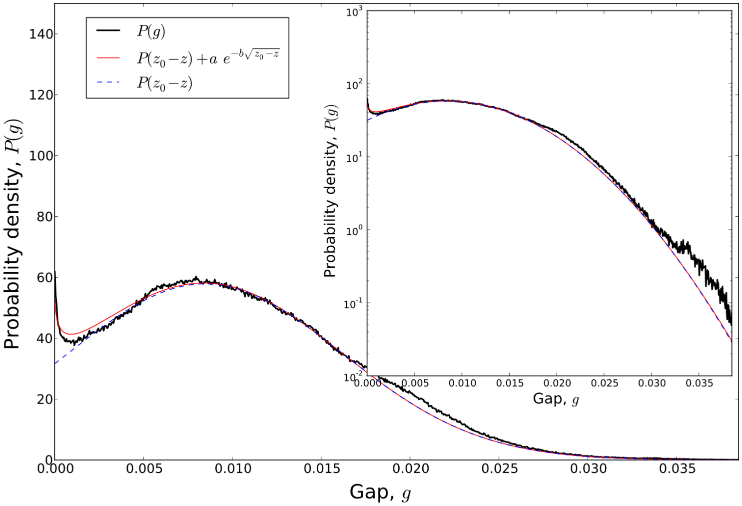

Area fraction $A' = 1.6\%$

Gap probability density VS geometrical overlap model (dashed line)
Near contact interface $P(g) \sim P(z_0 - z) + a \exp(-b\sqrt{z_0 - z})$

Solid contact results: gap distribution

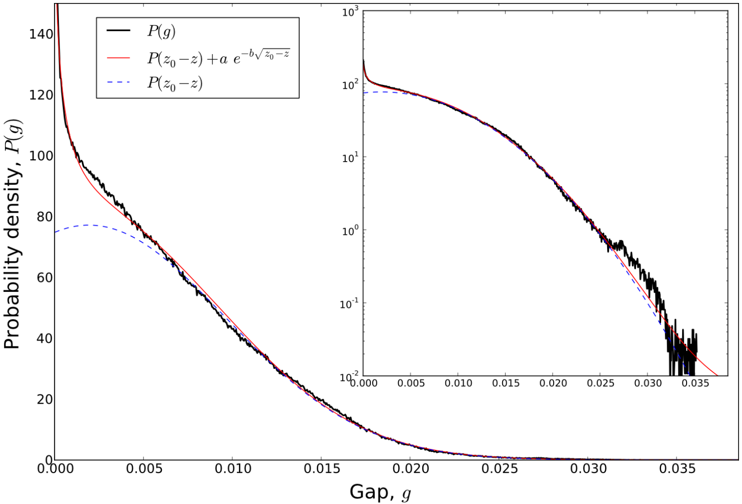

Area fraction $A' = 9.5\%$

Gap probability density VS geometrical overlap model (dashed line)
Near contact interface $P(g) \sim P(z_0 - z) + a \exp(-b\sqrt{z_0 - z})$

Solid contact results: gap distribution

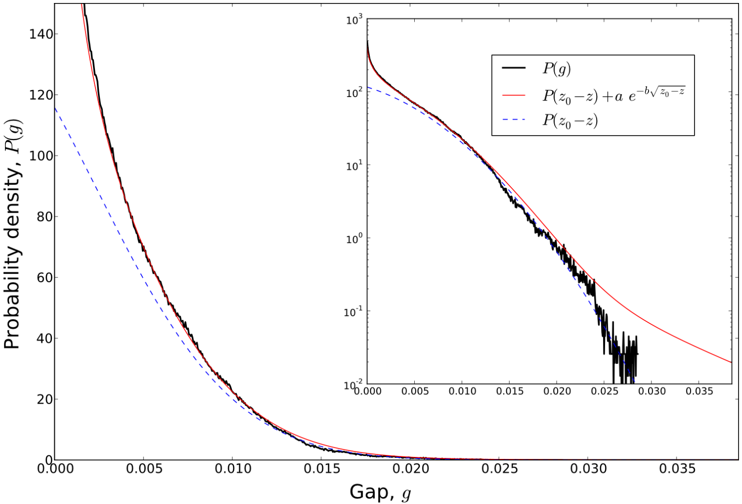

Area fraction $A' = 24\%$

Gap probability density VS geometrical overlap model (dashed line)
Near contact interface $P(g) \sim P(z_0 - z) + a \exp(-b\sqrt{z_0 - z})$

Solid contact results: gap distribution

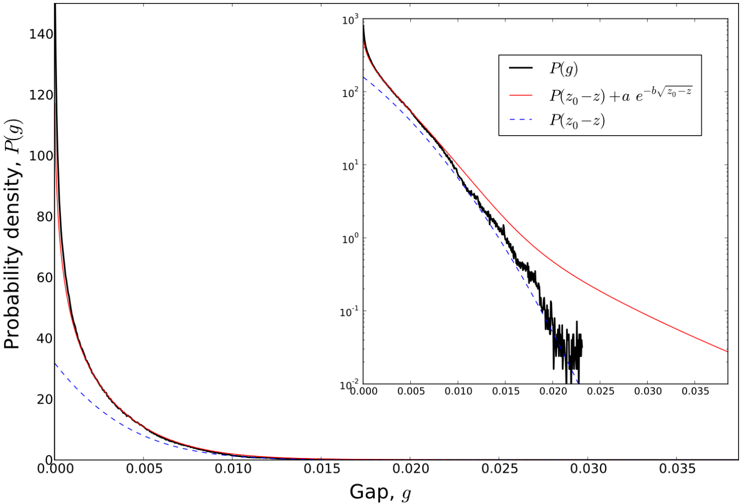

Area fraction $A' = 39\%$

Gap probability density VS geometrical overlap model (dashed line)
Near contact interface $P(g) \sim P(z_0 - z) + a\exp(-b\sqrt{z_0 - z})$

Geometrical overlap: morphology and percolation

- Geometrical overlap model is highly inaccurate[1,2]

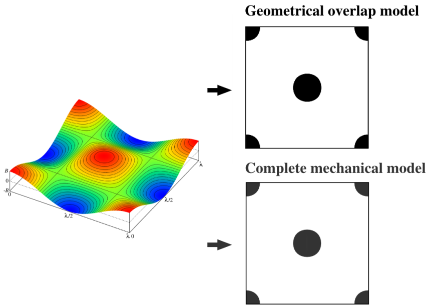

[1] Dapp, Lücke, Persson, Müser, *Phys. Rev. Lett.* 108 (2012)

[2] Yastrebov, Anciaux, Molinari. *Tribol Lett*, 56 (2014)

Geometrical overlap: morphology and percolation

- Geometrical overlap model is highly inaccurate[1,2]

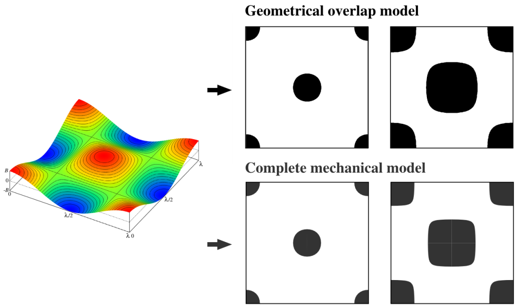

[1] Dapp, Lücke, Persson, Müser, *Phys. Rev. Lett.* 108 (2012)

[2] Yastrebov, Anciaux, Molinari. *Tribol Lett*, 56 (2014)

Geometrical overlap: morphology and percolation

- Geometrical overlap model is highly inaccurate[1,2]

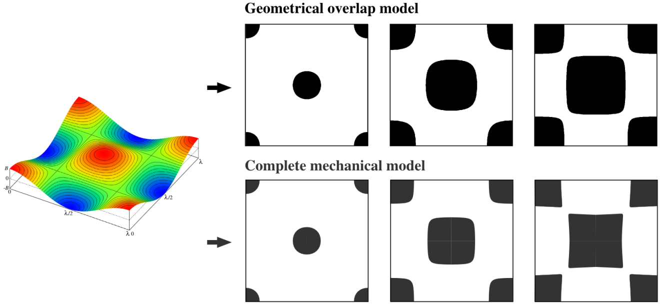

[1] Dapp, Lücke, Persson, Müser, *Phys. Rev. Lett.* 108 (2012)

[2] Yastrebov, Anciaux, Molinari. *Tribol Lett*, 56 (2014)

- Geometrical overlap model is highly inaccurate[1,2]

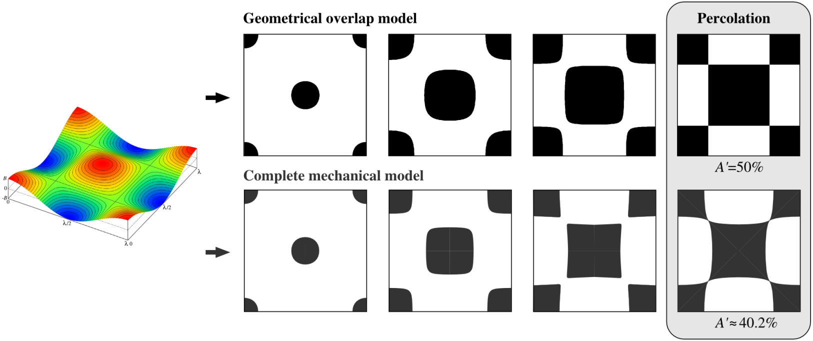

[1] Dapp, Lücke, Persson, Müser, *Phys. Rev. Lett.* 108 (2012)

[2] Yastrebov, Anciaux, Molinari. *Tribol Lett*, 56 (2014)

Creeping fluid transport

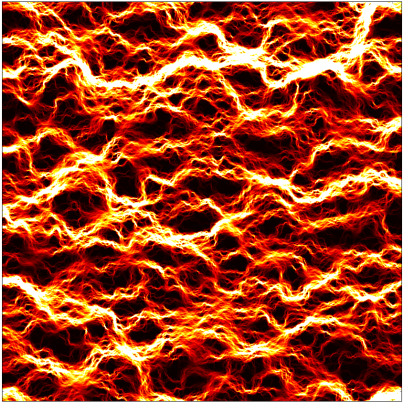

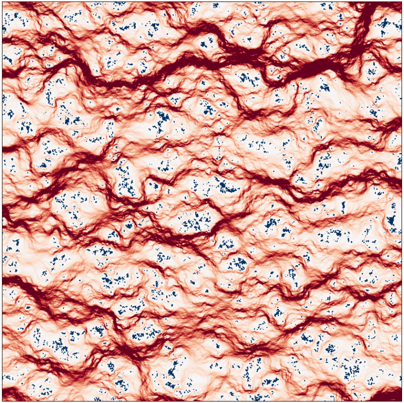

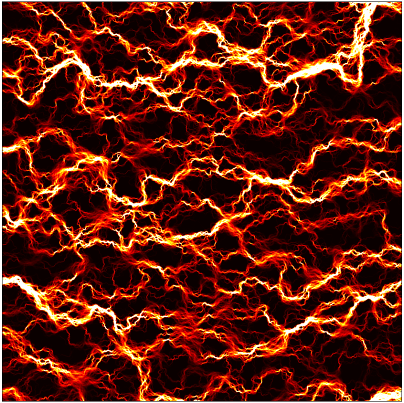

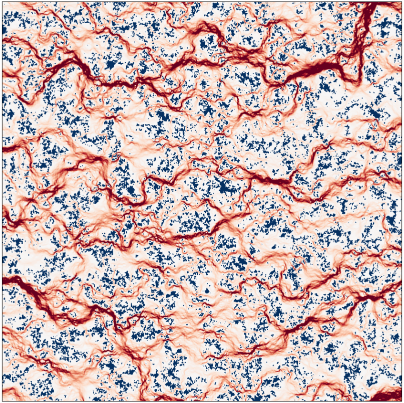

Creeping fluid transport

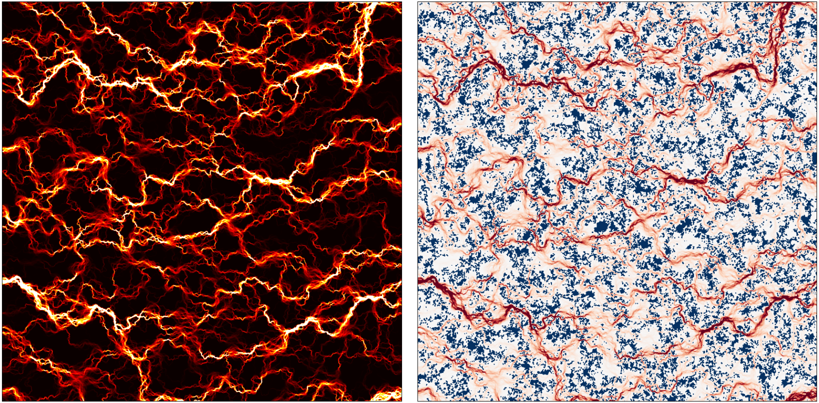

Creeping fluid transport

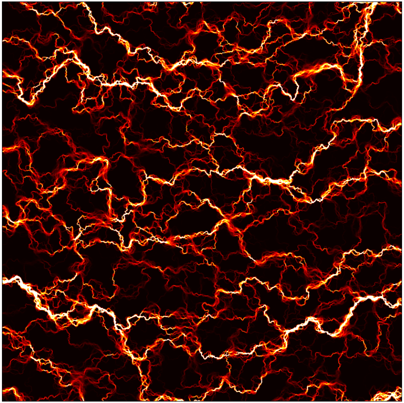

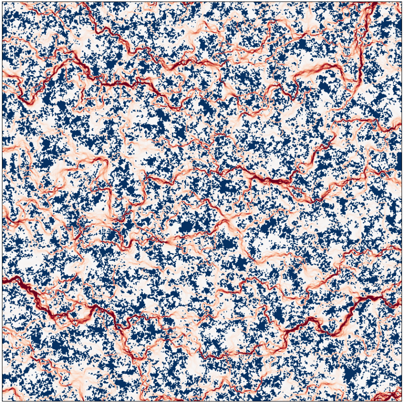

Creeping fluid transport

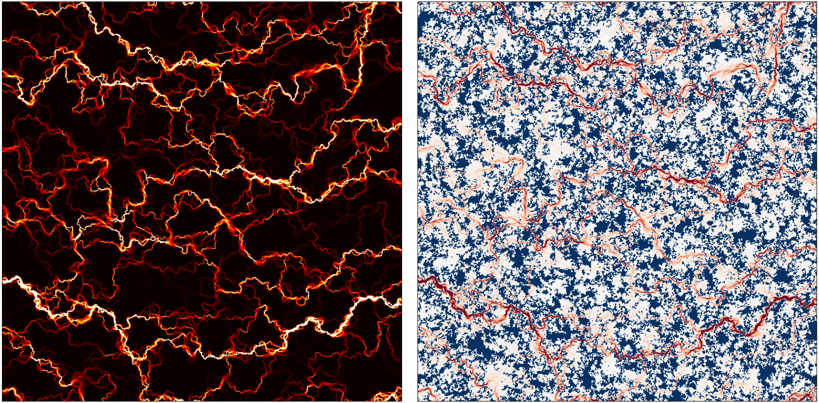

Creeping fluid transport

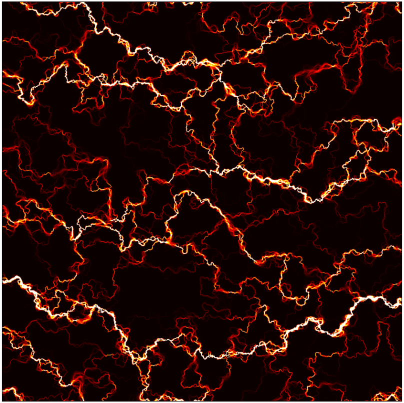

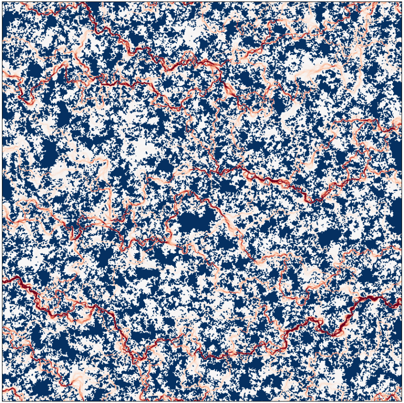

Creeping fluid transport

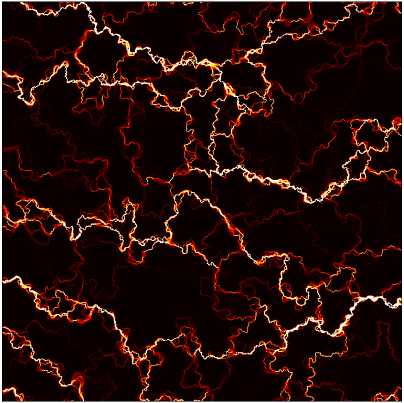
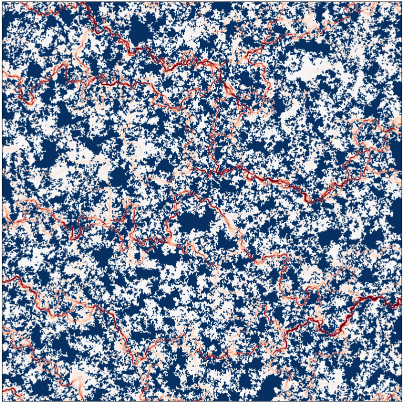

Creeping fluid transport

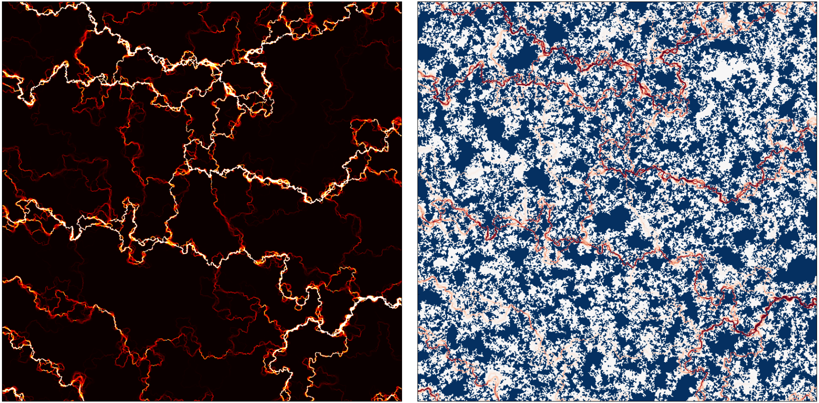

Creeping fluid transport

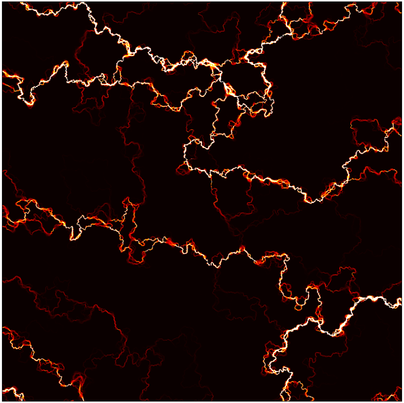

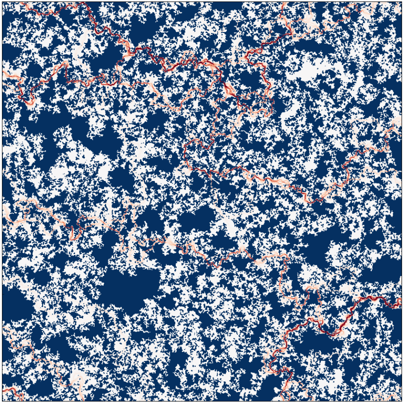

Creeping fluid transport

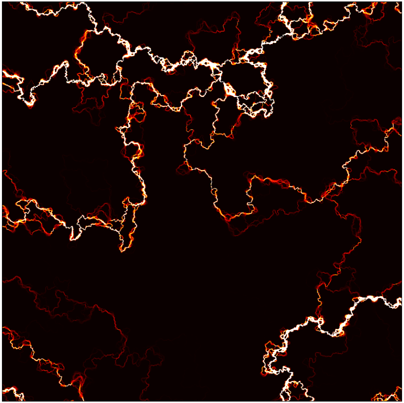

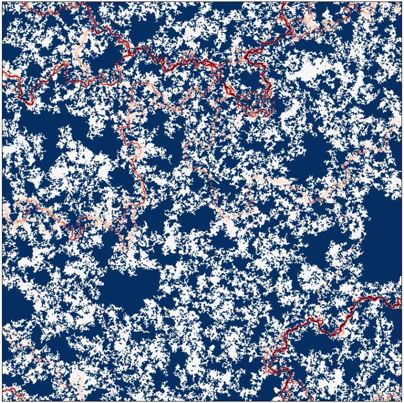

Creeping fluid transport

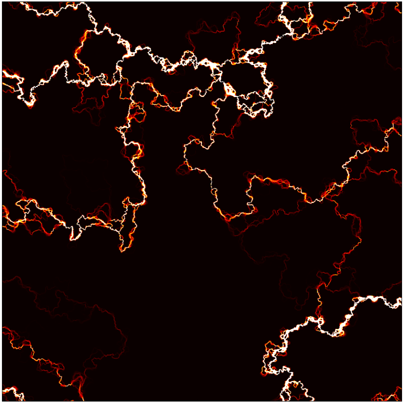

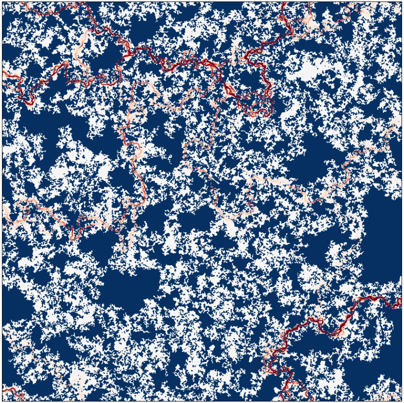

Creeping fluid transport

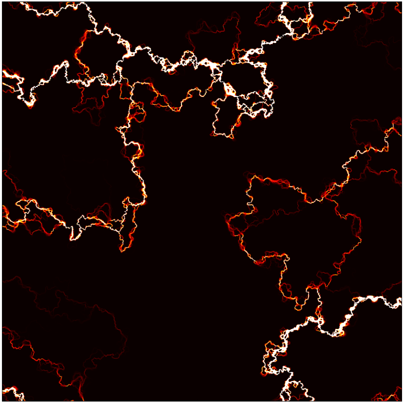

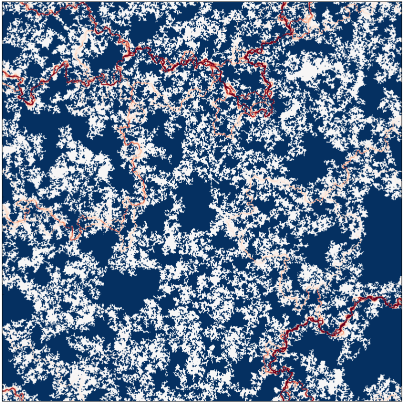

Creeping fluid transport

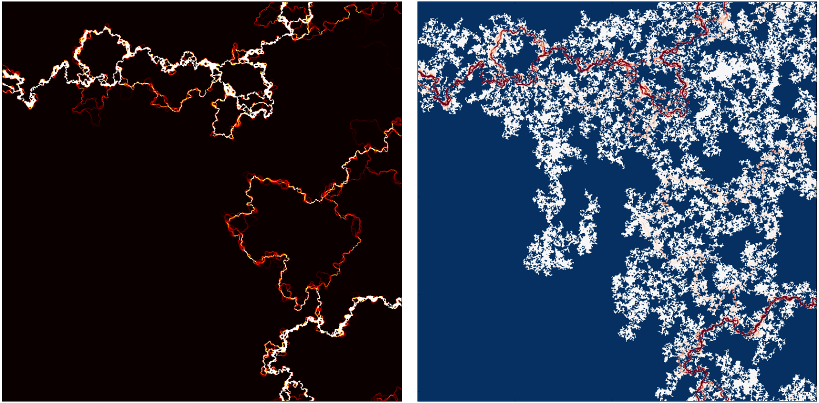

Contact area & trapped fluid

- Contact area does not conduct flow

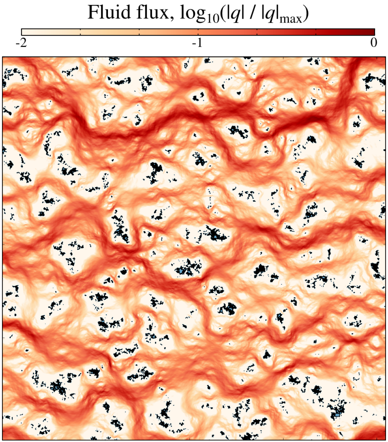

Fig. Fluid flux

Contact area & trapped fluid

- Contact area does not conduct flow

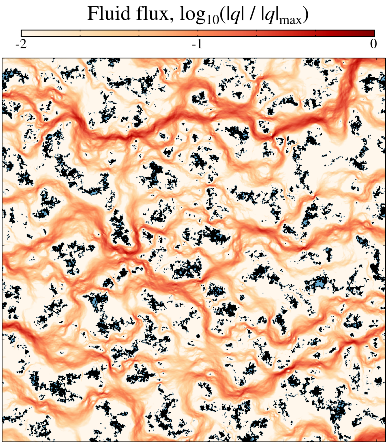

Fig. Fluid flux

- Contact area does not conduct flow

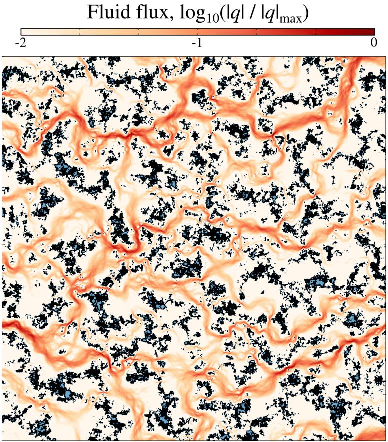

Fig. Fluid flux

Contact area & trapped fluid

- Contact area does not conduct flow

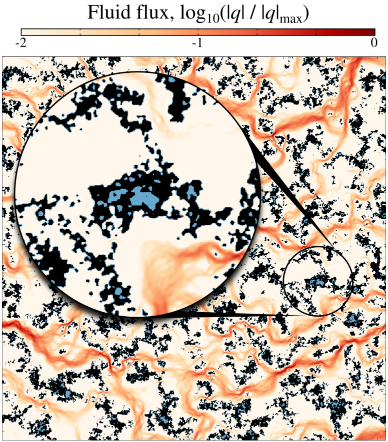

Fig. Fluid flux (zoom)

Contact area & trapped fluid

- Contact area does not conduct flow
- Islands of trapped fluid ≡ non-simply connected contact spots do not contribute to conduction
- Thus the effective transmissivity depends on the **effective contact area**:

$$A'_{\text{eff}} = A' + A'_t$$

A' is the contact area fraction
A'_t is the area of trapped fluid

- Effective medium transmissivity:

$$(1 - A') \int_0^\infty \frac{g^3 P(g)}{g^3 + K'_{\text{eff}} m_0^{3/2}}\, dg = \frac{1}{2}$$

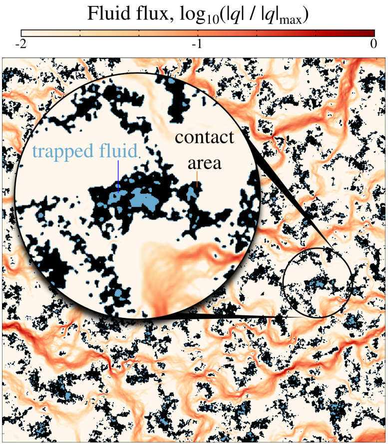

Fig. Fluid flux (zoom)

[1] Shvarts, Yastrebov. *Trapped Fluid in the Contact Interface*, JMPS:119 (2018)

Contact area & trapped fluid

- Contact area does not conduct flow
- Islands of trapped fluid ≡ non-simply connected contact spots do not contribute to conduction
- Thus the effective transmissivity depends on the **effective contact area**:

$$A'_{\text{eff}} = A' + A'_t$$

A' is the contact area fraction
A'_t is the area of trapped fluid

- Effective medium transmissivity:

$$(1 - A'_{\text{eff}}) \int\limits_0^\infty \frac{g^3 P(g)}{g^3 + K'_{\text{eff}} m_0^{3/2}}\, dg = \frac{1}{2}$$

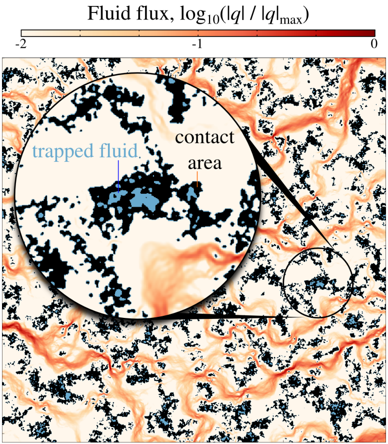

Fig. Fluid flux (zoom)

[1] Shvarts, Yastrebov. *Trapped Fluid in the Contact Interface*, JMPS:119 (2018)

Contact area & trapped fluid

- Contact area does not conduct flow
- Islands of trapped fluid ≡ non-simply connected contact spots do not contribute to conduction
- Thus the effective transmissivity depends on the **effective contact area**:

$$A'_{\text{eff}} = A' + A'_t$$

A' is the contact area fraction
A'_t is the area of trapped fluid

- Effective medium transmissivity:

$$(1 - A'_{\text{eff}}) \int\limits_0^\infty \frac{g^3 P(g)}{g^3 + K'_{\text{eff}} m_0^{3/2}}\, dg = \frac{1}{2}$$

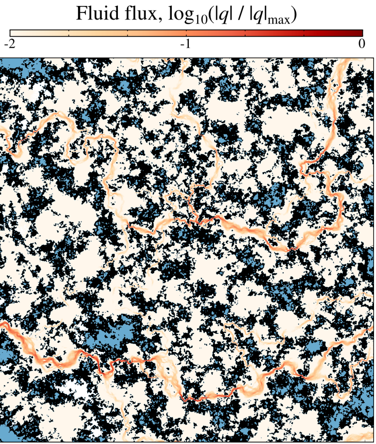

Fig. Fluid flux

[1] Shvarts, Yastrebov. *Trapped Fluid in the Contact Interface*, JMPS:119 (2018)

Contact area & trapped fluid

- Contact area does not conduct flow
- Islands of trapped fluid ≡ non-simply connected contact spots do not contribute to conduction
- Thus the effective transmissivity depends on the **effective contact area**:

$$A'_{\text{eff}} = A' + A'_t$$

A' is the contact area fraction
A'_t is the area of trapped fluid

- Effective medium transmissivity:

$$(1 - A'_{\text{eff}}) \int\limits_0^\infty \frac{g^3 P(g)}{g^3 + K'_{\text{eff}} m_0^{3/2}}\, dg = \frac{1}{2}$$

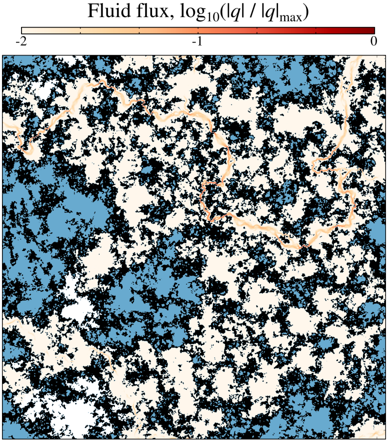

Fig. Fluid flux

[1] Shvarts, Yastrebov. *Trapped Fluid in the Contact Interface*, JMPS:119 (2018)

Contact area & trapped fluid

- Contact area does not conduct flow
- Islands of trapped fluid ≡ non-simply connected contact spots do not contribute to conduction
- Thus the effective transmissivity depends on the **effective contact area**:

$$A'_{\text{eff}} = A' + A'_t$$

A' is the contact area fraction
A'_t is the area of trapped fluid

- Effective medium transmissivity:

$$(1 - A'_{\text{eff}}) \int\limits_0^{\infty} \frac{g^3 P(g)}{g^3 + K'_{\text{eff}} m_0^{3/2}}\, dg = \frac{1}{2}$$

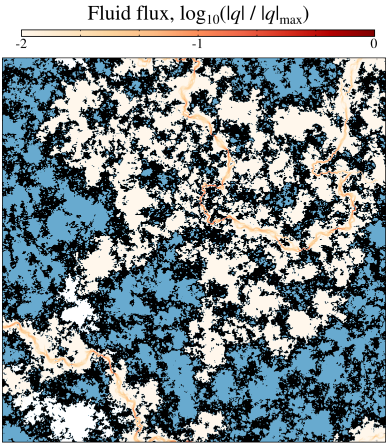

Fig. Fluid flux

[1] Shvarts, Yastrebov. *Trapped Fluid in the Contact Interface*, JMPS:119 (2018)

Effective contact area

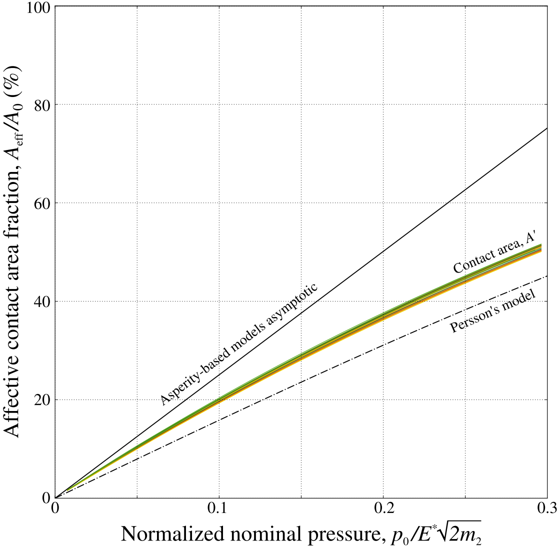

Effective contact area

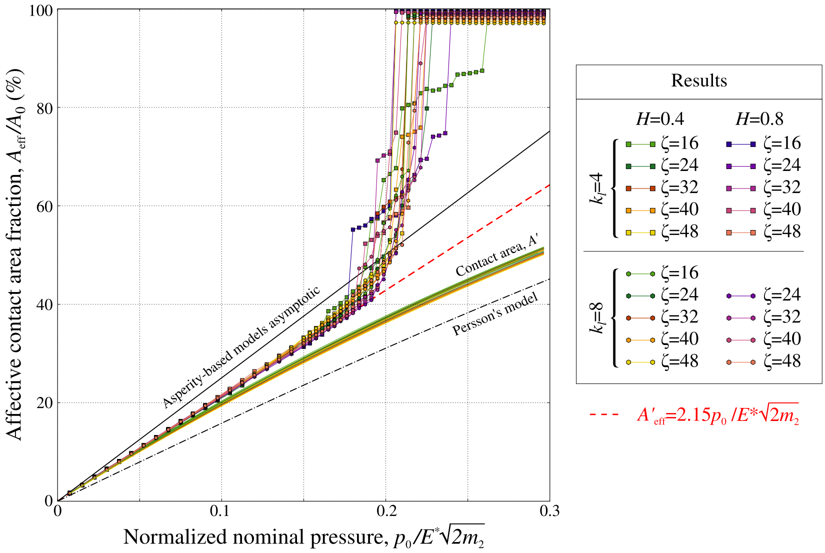

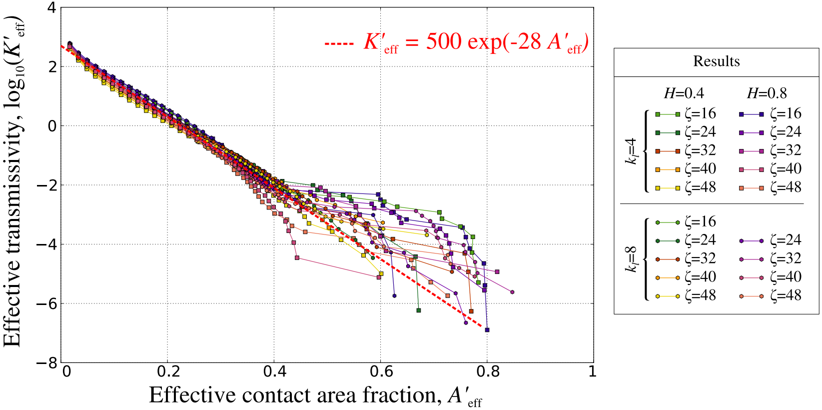

~ normalized nominal pressure p'

Fig. Evolution of the effective transmissivity

Effective transmissivity

- Effective area wrt load:

$$A'_{\text{eff}} \approx 2.15p'$$

- Normalized load:

$$p' = p_0/E^* \sqrt{2m_2}$$

- Normalized effective transmissivity wrt effective area:

$$K'_{\text{eff}} \approx 500 \exp(-28A'_{\text{eff}})$$

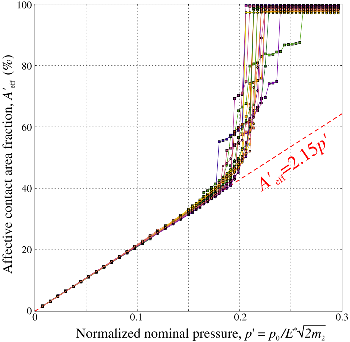

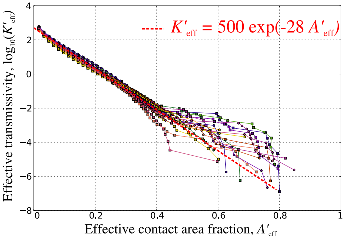

Effective transmissivity

- Effective area wrt load:

$$A'_{\text{eff}} \approx 2.15p'$$

- Normalized load:

$$p' = p_0/E^* \sqrt{2m_2}$$

- Normalized effective transmissivity wrt effective area:

$$K'_{\text{eff}} \approx 500 \exp(-28A'_{\text{eff}})$$

- Recall:

$$K'_{\text{eff}} = -\frac{12\mu\langle\, q_x \,\rangle L}{m_0^{3/2}\Delta P_f}$$

- Express the mean flow:

$$\langle\, q_x \,\rangle = -\frac{K'_{\text{eff}} m_0^{3/2}\Delta P_f}{12\mu L}$$

- Finally:

$$\boxed{\langle\, q_x \,\rangle \approx -\frac{41.7 \exp(-42.57 p_0/E^* \sqrt{m_2}) m_0^{3/2}\Delta P_f}{\mu L}}$$

Conclusion & current work

Main result:

Mean flow (far from the percolation) through contact of nominal area $L \times L$:

$$\langle\, q_x \,\rangle \approx -\frac{41.7 m_0{}^{3/2} \Delta P_f}{\mu L} \cdot \exp\left(-42.57 \frac{p_0}{E^* \sqrt{m_2}}\right)$$

u is dynamic viscosity,
ΔP_f is the pressure drop between the inlet and the outlet,
p_0 is the nominal applied pressure,
E^* is the effective elastic modulus.
Roughness parameters:
m_0 is the variance of roughness,
$2m_2$ is the variance of roughness gradient.

Conclusion & current work

Main result:

Mean flow (far from the percolation) through contact of nominal area $L \times L$:

$$\langle\, q_x \,\rangle \approx -\frac{41.7 {m_0}^{3/2} \Delta P_f}{\mu L} \cdot \exp\left(-42.57 \frac{p_0}{E^* \sqrt{m_2}}\right)$$

u is dynamic viscosity,
ΔP_f is the pressure drop between the inlet and the outlet,
p_0 is the nominal applied pressure,
E^* is the effective elastic modulus.
Roughness parameters:
m_0 is the variance of roughness,
$2m_2$ is the variance of roughness gradient.

Beyond the one-way coupling:

- Monolithic two-way FEM[1] framework coupling solid and fluid equations (thin flow, Reynolds equation) with contacts including islands of non-linear compressible fluid

[1] A.G. Shvarts, J. Vignollet, V.A. Yastrebov. "Computational framework for monolithic coupling for thin fluid flow in contact interfaces". Computer Methods in Applied Mechanics and Engineering, 379:113738 (2021).

General conclusion

The most critical assumption is the existence of the small wavelength cutoff

General conclusion

The most critical assumption is the existence of the small wavelength cutoff

- Fractal limit:
  Let $\lambda_s \to 0$, then $m_2 \to \infty$ and $\forall p_0 < \infty, A' \to 0$

General conclusion

The most critical assumption is the existence of the small wavelength cutoff

- Fractal limit:
  Let $\lambda_s \to 0$, then $m_2 \to \infty$ and $\forall p_0 < \infty, A' \to 0$
- Add some physics:
  Let $\lambda_s \sim$ Å, then $m_2 < C < \infty$ and $\forall p_0 > 0, A' > 0$

General conclusion

The most critical assumption is the existence of the small wavelength cutoff

- Fractal limit:
  Let $\lambda_s \to 0$, then $m_2 \to \infty$ and $\forall p_0 < \infty, A' \to 0$
- Add some physics:
  Let $\lambda_s \sim$ Å, then $m_2 < C < \infty$ and $\forall p_0 > 0, A' > 0$
- But, at Å-scales, continuum mechanics and especially continuum contact[1] do not work.

[1] Luan & Robbins. Nature 435 (2005).

General conclusion

The most critical assumption is the existence of the small wavelength cutoff

- Fractal limit:
  Let $\lambda_s \to 0$, then $m_2 \to \infty$ and $\forall p_0 < \infty, A' \to 0$
- Add some physics:
  Let $\lambda_s \sim$ Å, then $m_2 < C < \infty$ and $\forall p_0 > 0, A' > 0$
- But, at Å-scales, continuum mechanics and especially continuum contact[1] do not work.
- Search for relevant physics that could justify $\lambda_s \gg$ Å.
- Candidates: plasticity (scale dependent), surface energy and adhesion, interaction potential.

[1] Luan & Robbins. Nature 435 (2005).

☺ Thank you for your attention!